

Strong discontinuity formulations: a comparative study

J. Alfaiate

Instituto Superior Técnico and ICIST, Dept. Eng. Civil, Lisboa, Portugal

L. J. Sluys

Delft University of Technology, Dept. of Civil Eng. and Geosciences, Delft, The Netherlands

ABSTRACT: In this paper, the computational modelling of fracture in quasi-brittle materials is addressed. An embedded discontinuity methodology is presented, which is called the discrete strong discontinuity approach (Alfaiate and Sluys 2005). This formulation is derived within the scope of the strong discontinuity concept (Oliver et al. 2002); however, instead of considering fracture as a natural evolution from continuum damage, a discrete crack approach is adopted: the onset of fracture gives rise to the formation of a localized discontinuity, which can evolve from a zero width fictitious crack to a fully open stress-free crack.

The use of a pure discrete methodology was implemented by means of interface elements more than twenty years ago (Hillerborg et al. 1976), (Bocca et al. 1986). In spite of the drawbacks of this approach whenever the crack path is not known in advance, it is still known to be most numerically reliable for prescribed crack-ing. This is why this formulation is still being used nowadays, for instance, to model the interface behaviour between two materials, such as with masonry, the internal concrete-steel adhesion or the external concrete-FRP reinforcement.

Recently, a new technique has been used to model fracture, known as the extended finite element method (Möes et al. 1999). In this paper a comparison of these different strong discontinuity descriptions is given. Several simple examples obtained at element level are first presented, with the purpose of clearly illustrating the differences between the discrete-interface, the discrete strong discontinuity and the extended finite element approaches. Next, towards a unified view of these different strong discontinuity descriptions, a better approximation of the kinematics of the element ahead of the crack tip is proposed, common to both the discrete strong discontinuity approach and the extended finite element method.

1 INTRODUCTION

In this paper, three different strong discontinuity descriptions are compared: the discrete-interface, the discrete strong discontinuity method and the extended finite element method. All these formulations aim to approximate the same problem, which consists of a continuum crossed by a discontinuity Γ_d , dividing Ω into two parts: Ω^+ and Ω^- . This discontinuity can be interpreted as an internal boundary where the tractions \mathbf{t}^+ and \mathbf{t}^- are applied. In the discrete-interface approach, interface elements located at interelement boundaries are used to model the discontinuity. With this formulation we get: *i*) mesh objectivity with prescribed cracks and *ii*) a true representation of strong discontinuities. Nevertheless, it is well known that with non-prescribed cracks, either remeshing must be performed (Ingraffea 1989) or approximated crack paths are obtained (Alfaiate et al. 1997).

In the embedded discontinuity approach (Simo and Rifai 1990), (Simo et al. 1993), (Armero and Garikipati 1996), (Oliver 1996): *i*) the additional degrees of freedom are local to each parent element, *ii*) constant jumps are adopted across each element *iii*) traction continuity is imposed in the strong form, although in average, which gives rise to *iv*) a non-symmetric formulation. Later, Sancho et al. (2005) developed a consistent weak symmetric formulation in which: *i*) constant jumps still are adopted across each parent element, but *ii*) no tracking of the crack path is enforced. As a consequence, the crack crosses the parent element in an *optimal* manner so that the element can properly accommodate the additional deformation, avoiding the locking problems obtained in the former embedded formulation.

Alfaiate and Sluys (2005), developed a third embedded formulation designated as the discrete strong

discontinuity approach (DSDA), in which: *i*) a weak symmetric consistent form is also used, *ii*) the additional degrees of freedom are global, *iii*) non-homogeneous jumps are adopted in each parent element and *iv*) both the crack path and the jumps are continuous across element boundaries.

Finally, in the extended finite element method (XFEM) a consistent weak form is still used, but Ω^+ and Ω^- are modelled using two element layers on top of each other (Möes et al. 1999), (Duarte et al. 2000), (Wells and Sluys 2001), (Simone et al. 2003): *i*) in each parent element the degrees of freedom are doubled, *ii*) the additional degrees of freedom are global, *iii*) continuous jumps as well as crack paths across element boundaries are obtained and *iv*) this formulation is within the scope of the generalized finite element method.

It has been often said that the extended finite element method is superior to the embedded discontinuity approach. Oliver et al. (2006) made a comparison between the former non-symmetric embedded formulation and the extended finite element method and they did not find that much difference. Here, another comparison is made, this time among the discrete strong discontinuity approach, the extended finite element method and the discrete-interface approach. For that purpose, the variational formulation is first briefly reviewed; next, trying to better understand the *whys* in detail, the numerical implementation will be presented in a very simple way, at the element level. Finally, some simple academic examples are presented.

2 KINEMATICS and VARIATIONAL FORMULATION

The kinematics of both the discrete strong discontinuity approach and the extended finite element method can be presented in a common framework: it is usual to assume that the total displacement \mathbf{u} is obtained as the sum of the regular part $\hat{\mathbf{u}}$ in the bulk and the displacement jump $[[\mathbf{u}]]$ which is transmitted to Ω^+ using the heaviside function:

$$\mathbf{u}(\mathbf{x}) = \hat{\mathbf{u}}(\mathbf{x}) + \mathcal{H}_{\Gamma_d} \tilde{\mathbf{u}}, \quad (1)$$

where \mathcal{H}_{Γ_d} is the heaviside function and $\tilde{\mathbf{u}}$ are additional displacements induced by the jump, such that

$$[[\mathbf{u}]] = \tilde{\mathbf{u}}|_{\Gamma_d}. \quad (2)$$

The variational formulation used for the three strong discontinuity approaches has been derived in various ways. For instance, in the extended finite element method, Simone (2003) considers the discontinuity as an internal boundary and imposes separately the principle of virtual work on Ω and Ω^+ , whereas Wells (2001) used the properties of the dirac

delta function to obtain the energy in the discontinuity. Here, the variational formulation for all these discrete approaches is presented in a very simple format which is usually adopted in the discrete-interface approach. Consider the principle of virtual work, take the strain energy $\int_{\Omega \setminus \Gamma_d} (\nabla^s \delta \mathbf{u}) : \boldsymbol{\sigma}(\boldsymbol{\varepsilon}) d\Omega$, the external work $\int_{\Omega \setminus \Gamma_d} \delta \mathbf{u} \cdot \mathbf{b} d\Omega + \int_{\Gamma_t} \delta \mathbf{u} \cdot \bar{\mathbf{t}} d\Gamma$ (these are the usual terms in a continuum approach) and add the term corresponding to the work done in the discontinuity $\int_{\Gamma_d} \delta [[\mathbf{u}]] \cdot \mathbf{t}^+ d\Gamma$. We obtain:

$$\begin{aligned} & - \int_{\Omega \setminus \Gamma_d} (\nabla^s \delta \mathbf{u}) : \boldsymbol{\sigma}(\boldsymbol{\varepsilon}) d\Omega + \int_{\Omega \setminus \Gamma_d} \delta \mathbf{u} \cdot \mathbf{b} d\Omega \\ & + \int_{\Gamma_t} \delta \mathbf{u} \cdot \bar{\mathbf{t}} d\Gamma + \int_{\Gamma_d} \delta [[\mathbf{u}]] \cdot \mathbf{t}^+ d\Gamma = 0, \end{aligned} \quad (3)$$

where (\cdot) and $(:)$ refer to single and double contractions, respectively. In fact, this variational formulation was already presented in Malvern (1969) and still applies to all three formulations studied here.

3 NUMERICAL IMPLEMENTATION

If we decouple the work in the bulk from the work in the discontinuity, we obtain two equations. Incrementally, upon discretization, we get:

$$\mathbf{K}_{aa}^e d\hat{\mathbf{a}}^e = d\mathbf{f}_{ext}^e \quad (4)$$

$$\mathbf{K}_d d\mathbf{w}^e = d\mathbf{f}_{w,ext}^e \quad (5)$$

where $\hat{\mathbf{a}}$ are the regular degrees of freedom used to approximate $\hat{\mathbf{u}}$, \mathbf{w} are the degrees of freedom used to approximate the jumps $[[\mathbf{u}]]$,

$$\mathbf{K}_{aa}^e = \int_{\Omega^e} \mathbf{B}^{eT} \mathbf{D}^e \mathbf{B}^e d\Omega, \quad (6)$$

$$\mathbf{K}_d^e = \int_{\Gamma_d^e} \mathbf{N}_w^{eT} \mathbf{T}^e \mathbf{N}_w^e d\Gamma, \quad (7)$$

$$d\mathbf{f}_{ext}^e = \int_{\Omega^e} \mathbf{N}^{eT} d\mathbf{b}^e d\Omega + \int_{\Gamma_t^e} \mathbf{N}^{eT} d\bar{\mathbf{t}}^e d\Gamma, \quad (8)$$

and $d\mathbf{f}_{w,ext}^e$ is the external force vector applied to the discontinuity. In equation (7), \mathbf{N}_w^e are the shape functions used to interpolate the jumps along the discontinuity lines Γ_d and \mathbf{T} is the constitutive matrix adopted for the discontinuity, i.e.,

$$d\mathbf{t}^e = \mathbf{T} [[\mathbf{u}]] = \mathbf{T} \mathbf{N}_w^e d\mathbf{w}^e \quad (9)$$

This approximation is particularly suited to the discrete-interface approach, in which the jumps are obtained at separate interface elements. The other two approaches actually differ in the way the discontinuity is represented.

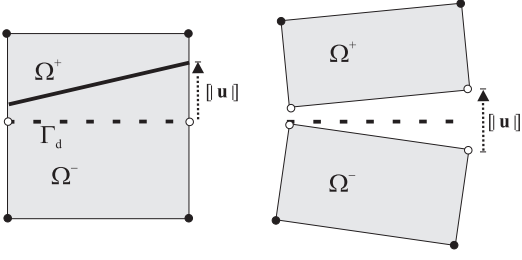


Figure 1: DSDA: mode-I discontinuity

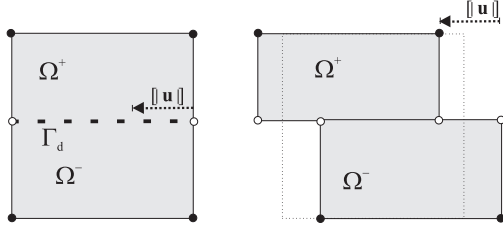


Figure 2: DSDA: mode-II discontinuity

In the discrete strong discontinuity approach these equations still apply since the discontinuity is embedded as if it was an interface. In figs.1 and 2 the black nodes are the regular nodes and the white nodes are the additional jump nodes. In order to evaluate the total displacements \mathbf{u} , the jumps are transmitted to the regular nodes as a rigid body motion:

$$\mathbf{u}^e = \mathbf{N}^e(\hat{\mathbf{a}}^e + \mathcal{H}_{\Gamma_d}\tilde{\mathbf{a}}) = \mathbf{N}^e(\hat{\mathbf{a}}^e + \mathcal{H}_{\Gamma_d}\mathbf{M}_w^e\mathbf{w}), \quad (10)$$

where $\tilde{\mathbf{a}}$ are the additional nodal displacements induced by the jumps and matrix \mathbf{M}_w^e gives rise to a rigid-body motion of Ω^{e+} over Ω^{e-} (Alfaiate and Sluys 2005).

In the extended finite element method, the degrees of freedom are doubled, since the enrichment is provided by a second element layer (see figs.3 and 4). Thus, the total continuum displacements $\hat{\mathbf{u}}$ are now the sum of the displacements from the two layers:

$$\hat{\mathbf{u}}^e = \mathbf{N}^e(\hat{\mathbf{a}}_1^e + \mathcal{H}_{\Gamma_d}\hat{\mathbf{a}}_2^e), \quad (11)$$

where $\hat{\mathbf{a}}_1^e$ and $\hat{\mathbf{a}}_2^e$ are the regular part obtained at the first and second layer, respectively, the latter subjected to:

$$\hat{\mathbf{a}}_2^e = \mathbf{0} \text{ at } \Gamma_d. \quad (12)$$

Thus, we obtain,

$$\begin{aligned} \mathbf{u}^e &= \hat{\mathbf{u}}^e + \mathcal{H}_{\Gamma_d}\tilde{\mathbf{u}}^e \\ &= \mathbf{N}^e[\hat{\mathbf{a}}_1^e + \mathcal{H}_{\Gamma_d}(\hat{\mathbf{a}}_2^e + \tilde{\mathbf{a}}^e)] \text{ in } \Omega \setminus \Gamma_d. \end{aligned} \quad (13)$$

Note that, according to this interpretation, from equation (13) it is clear that the degrees of freedom $\tilde{\mathbf{a}}$ remain a rigid-body motion projection of the jumps, exactly the same way as done with the discrete strong discontinuity approach. In fact, due to equations (12) and (2), we obtain:

$$\tilde{\mathbf{u}}|_{\Gamma_d} = \mathbf{N}|_{\Gamma_d}\tilde{\mathbf{a}}. \quad (14)$$

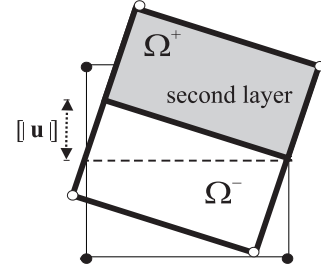


Figure 3: X-FEM: mode-I

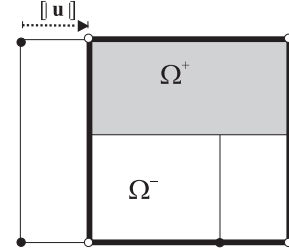


Figure 4: X-FEM: mode-II discontinuity

Furthermore, due to equation (12) and since $\mathbf{B}\tilde{\mathbf{a}} = \mathbf{0}$, the usual coupled element equations in the extended finite element method (Wells 2001), (Simone 2003):

$$\mathbf{K}_{aa}^e d\mathbf{a}^e + \mathbf{K}_{aa}^{+e} d\mathbf{b}^e = d\mathbf{f}_{ext}^e \quad (15)$$

$$\mathbf{K}_{aa}^{+e} d\mathbf{a}^e + (\mathbf{K}_{aa}^{+e} + \mathbf{K}_d^e) d\mathbf{b}^e = d\mathbf{f}_{ext}^{+e}$$

become:

$$\mathbf{K}_{aa}^e d\hat{\mathbf{a}}_1^e + \mathbf{K}_{aa}^{+e} d\hat{\mathbf{a}}_2^e = d\mathbf{f}_{ext}^e \quad (16)$$

$$\mathbf{K}_{aa}^{+e} d\hat{\mathbf{a}}_1^e + \mathbf{K}_{aa}^{+e} d\hat{\mathbf{a}}_2^e + \mathbf{K}_d^e d\tilde{\mathbf{a}}^e = d\mathbf{f}_{ext}^{+e}$$

At this stage, three main conclusions can be drawn:

1. due to the separation of the $\hat{\mathbf{a}}^e \in \Omega$ into $(\hat{\mathbf{a}}_1^e \in \Omega$ and $\hat{\mathbf{a}}_2^e \in \Omega^+)$, the difference between these two discretizations lies in the bulk:

$$\Delta\hat{\mathbf{a}}^e = \begin{cases} \hat{\mathbf{a}}_1^e - \hat{\mathbf{a}}^e & \text{if } \mathbf{x} \in \Omega^- \\ \hat{\mathbf{a}}_1^e + \hat{\mathbf{a}}_2^e - \hat{\mathbf{a}}^e & \text{if } \mathbf{x} \in \Omega^+; \end{cases} \quad (17)$$

2. as a consequence, the gradient of the additional displacements $\hat{\mathbf{a}}_2^e$ in Ω^+ is non-zero, which is the *only* reason why separate integration on Ω^+ becomes necessary;
3. the kinematics of the discrete strong discontinuity approach may be considered as a particular case of the extended finite element method in which $\hat{\mathbf{a}}_2^e$ drops, giving rise to a rigid second layer.

Two extreme situations can be defined: *i*) either the discontinuity is much softer than the bulk – this is the usual case when we model a crack or a shear band; or *ii*) the discontinuity is much stiffer than the bulk.

In the following section some simple examples at element level are presented using the three descriptions.

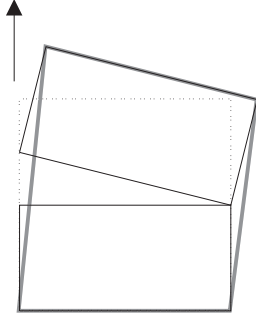


Figure 5: Mode-I: soft discontinuity

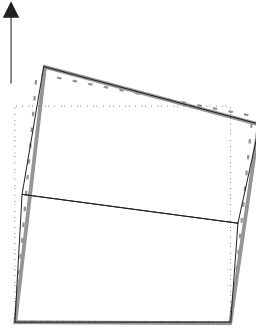


Figure 6: Mode-I: soft bulk

4 EXAMPLES

Consider the case presented in fig.5, in which we have a mode-I example and the discontinuity is much softer than the bulk (Young modulus $E=10^3$ GPa, normal discontinuity stiffness $T=1$ MPa/mm). With the discrete-interface approach we obtain the configuration in black; the extended finite element method and the discrete strong discontinuity approach configurations are both in grey and practically coincide.

Now, if the discontinuity is much stiffer than the bulk, (Young modulus $E=10$ MPa, normal discontinuity stiffness $T=1000$ MPa/mm) the differences become more important due to the additional bulk deformation. In fig.6, the discrete-interface configuration is represented in black, the extended finite element method is plain grey and the discrete strong discontinuity approach is dashed grey.

Consider again the example of fig.5. If Ω^+ tends to zero, the differences between the DSDA and the X-FEM results decrease even further (see fig.7).

In mode-II the conclusions are similar; in fig.8,

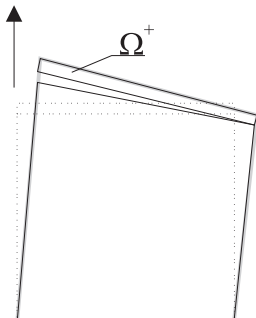


Figure 7: Mode-I: soft discontinuity

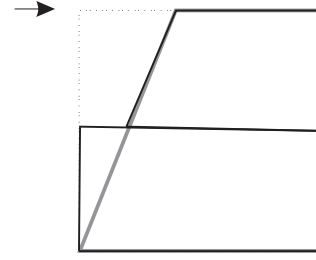


Figure 8: Mode-II: soft discontinuity

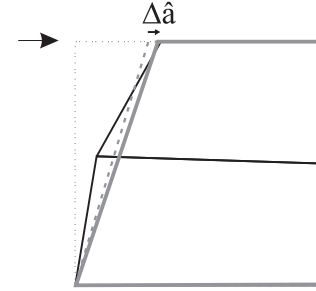


Figure 9: Mode-II: soft bulk

we see the results obtained with a soft shear band, whereas in fig.9 the results obtained with a stiff shear band are presented. In this example the difference between the regular displacement fields in the DSDA and the X-FEM, $\Delta \hat{a}$, is marked.

From these simple examples it is possible to conclude that:

- i. for normal cracks or shear bands, in which case the discontinuities are much softer than the bulk, the results obtained from these two formulations (DSDA and X-FEM) are essentially the same and the nodal displacements practically coincide with those obtained with the discrete-interface approach;
- ii. in the opposite case, in which the discontinuity is much stiffer than the bulk, the X-FEM gives rise to nodal displacements closer than the DSDA to the ones obtained with the discrete-interface approach.

The latter conclusion emphasizes the fact that, in the X-FEM, there is an inherent bulk refinement, which can be interpreted as a particular case of *mesh refinement*. In fact, the superposition of the two layers in the bulk can better approximate the solution obtained with two different elements, as done with the discrete-interface approach.

Nevertheless, if the discontinuity is much stiffer than the bulk, we might distinguish three possibilities: *a)* the continuum is crossed by a stiff inclusion, *b)* the discontinuity is submitted to compressive stresses and the constitutive relation is penalized in order to avoid overlapping, or *c)* there is no reason to insert a discontinuity in the first place! Indeed, we should keep

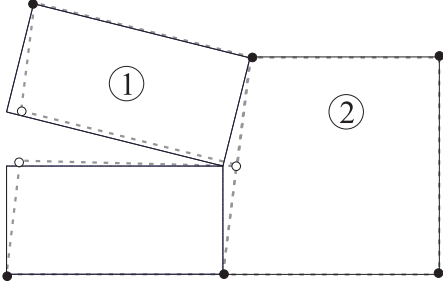


Figure 10: soft discontinuity: discrete-interface vs DSDA

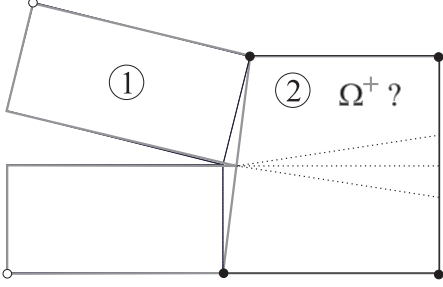


Figure 11: soft discontinuity: discrete-interface vs X-FEM

in mind that both the DSDA and the X-FEM are element enrichment techniques, which were built aiming to approximate softening; within this scope, both descriptions give rise to similar results.

Now let us look once more to the first mode-I example in more detail. If the real deformation of the elements is taken into account the results are described below: in fig.10 the configuration obtained with both the discrete-interface and the DSDA are presented, whereas in fig.11 the configuration obtained with both the discrete-interface and the X-FEM are presented. Again, the discrete-interface is represented in black, the DSDA is represented in dashed grey and the X-FEM in plain grey. Although in the first element the energy in all situations is practically the same (it would be exactly the same if the bulk was rigid), that is not the case in the second element. Element number 2 should deform according to the discrete-interface approach; however, neither the DSDA nor the X-FEM can model this behaviour (note that with the X-FEM, the right additional nodes, lying on the tip edge, are inactive). This fact may influence the stress field near the crack tip, thus it may have consequences for the evolution of the discontinuity. However, in order to allow the second element to deform properly, we need to define Ω^+ (see fig.11), and this we do not know yet!

Here an approximation for this problem is proposed, which can be regarded as common to both the DSDA and the X-FEM. First, let us assume a position for Γ_d , as represented in fig.12 (with the corresponding definition of Ω^+). In this figure, the second layer obtained with the X-FEM is represented in grey. Based on the location of the additional nodes adja-

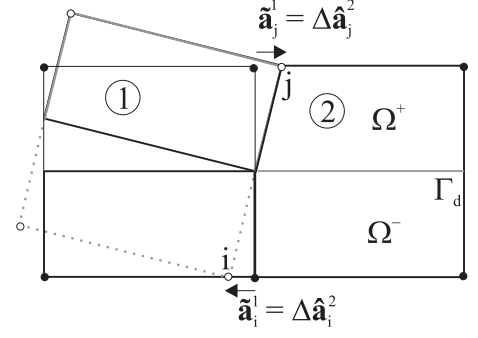


Figure 12: An approximation to the correct deformation of element 2

cent to the tip (nodes i and j marked in white), we know that the *lacking* displacement field in the second element, $\Delta \hat{\mathbf{u}}^{(2)}(\mathbf{x})$, is equal to the additional displacement field obtained for the first element, $\tilde{\mathbf{u}}^{(1)}(\mathbf{x})$, i.e.,

$$\Delta \hat{\mathbf{a}}^{(2)} = \begin{cases} \tilde{\mathbf{a}}^{(1)} & \text{if nodes lie at tip edge} \\ \mathbf{0} & \text{otherwise.} \end{cases} \quad (18)$$

As a consequence, instead of equations (6) and (7) in the DSDA or equations (15) in the X-FEM, we can write the following for the second element:

$$\mathbf{K}_{aa}^{(2)} d\hat{\mathbf{a}} = d\mathbf{f}_{ext}^{(2)} - \mathbf{K}_{aa}^{+(2)} d\Delta \hat{\mathbf{a}}^{(2)} = d\mathbf{f}_{ext}^{*(2)} \quad (19)$$

$$d\mathbf{w}^{(2)} \text{ (or } d\tilde{\mathbf{a}}^{(2)}) = \mathbf{0}.$$

Note that no additional degrees of freedom are introduced in this formulation; however, separate integration on Ω^+ becomes necessary in the second element. The introduction of this new approach should approximate both the DSDA and the X-FEM from the discrete-interface description and might be interpreted as a contribution towards a unified view of all three strong discontinuity formulations.

5 CONCLUSIONS

In this paper a comparative study of three strong discontinuity formulations is presented, namely the discrete-interface approach, the discrete strong discontinuity approach and the extended finite element method. Towards a unified view of these different discontinuity descriptions, some shared properties can be put forward, namely:

1. they can be built upon the same variational formulation;
2. the kinematics of the DSDA can be interpreted as a particular case of the kinematics of the X-FEM in which the second element layer is rigid;
3. XFEM exhibits better kinematics of the bulk, closer to the kinematics obtained with the discrete-interface approach,

4. but both the DSDA and the X-FEM give rise to similar results for one element crossed by a soft discontinuity;
5. both the X-FEM and the DSDA provide *exactly* the same description of softening behaviour within a strong discontinuity;
6. it is possible to better approximate the kinematics of the element ahead of the tip in a common way for both the DSDA and the X-FEM descriptions without the need to increase the number of degrees of freedom, although sub-integration on Ω^+ becomes necessary.

Some main different characteristics can also be advanced, such as:

1. the DSDA can not be considered a particular case of the X-FEM since it is built on a different background – the DSDA is an embedded approach, built at element level, whereas the X-FEM is built at nodal level;
2. in the X-FEM more degrees of freedom are needed than in the DSDA;
3. in the X-FEM, sub-integration on Ω^+ is only needed to evaluate a part of the bulk displacement field, i.e., $\hat{\mathbf{a}}_2$;
4. this sub-integration could be interpreted as a sort of remeshing, although certainly more benign than the usual one since no additional elements are defined;
5. in the DSDA no sub-integration on Ω^+ is necessary;
6. the X-FEM can lead to numerical integration problems along the discontinuity Γ_d , which is not the case with the DSDA (Simone 2004);
7. in the DSDA, additional nodes are located at the discontinuity, where the quantities of interest are to be measured, giving rise to a straight physical interpretation of the additional degrees of freedom;
8. due to (7), problems in which boundary conditions must be introduced at Γ_d , like moisture or the injection of epoxy resin to repair cracks, benefit from such implementation.

REFERENCES

- Alfaiate, J., E. B. Pires, and J. A. C. Martins (1997). A finite element analysis of non-prescribed crack propagation in concrete. *Computers and Structures* 63(1), 17–26.
- Alfaiate, J. and L. Sluys (2005). Discontinuous numerical modelling of fracture using embedded discontinuities. In D. R. J. Owen, E. O. nate, and B. Suárez (Eds.), *Computational Plasticity, Fundamentals and Applications, COMPLAS VIII*, Barcelona, Spain.
- Armero, F. and K. Garikipati (1996). An analysis of strong discontinuities in multiplicative finite strain plasticity and their relation with the numerical simulation of strain localization. *International Journal of Solids and Structures* 33(20–22), 2863–2885.
- Bocca, P., A. Carpinteri, and S. Valente (1986). Mixed mode fracture of concrete. *International Journal of Solids and Structures* 27, 1139–1153.
- Duarte, C. A., I. Babuška, and J. T. Oden (2000). Generalized finite element methods for three-dimensional structural mechanics problems. *Computers and Structures* 77(2), 215–232.
- Hillerborg, A., M. Modeer, and P. E. Petersson (1976). Analysis of crack formation and crack growth in concrete by means of fracture mechanics and finite elements. *Cement and Concrete Research* 6(6), 773–782.
- Ingraffea, A. (1989). Shear cracks. In L. Elfgren (Ed.), *Fracture mechanics of concrete structures - from theory to applications, report of the Technical Committee 90-FMA Fracture Mechanics of Concrete-Applications*, pp. 231–233. London, United Kingdom: Chapman and Hall.
- Malvern, L. E. (1969). *Introduction to the Mechanics of a Continuous Medium*. New Jersey: Prentice-Hall International.
- Möes, N., J. Dolbow, and T. Belytschko (1999). A finite element method for crack growth without remeshing. *International Journal for Numerical Methods in Engineering* 46(1), 131–150.
- Oliver, J. (1996). Modelling strong discontinuities in solid mechanics via strain softening constitutive equations. Part 1: Fundamentals. *International Journal for Numerical Methods in Engineering* 39(21), 3575–3600.
- Oliver, J., A. E. Huespe, M. D. G. Pulido, and E. Chaves (2002). From continuum mechanics to fracture mechanics: the strong discontinuity

- approach. *Engineering Fracture Mechanics* 69, 113–136.
- Oliver, J., A. E. Huespe, and P. J. Sánchez (2006). A comparative study on finite elements for capturing strong discontinuities: E-fem vs x-fem. *Computer Methods in Applied Mechanics and Engineering* 195, 4732–4752.
- Sancho, J., J. Planas, J. Gálvez, D. Cendón, and A. Fathy (2005). Three-dimensional simulation of concrete fracture using embedded crack elements without enforcing crack path continuity. In D. R. J. Owen, E. O. nate, and B. Suárez (Eds.), *Computational Plasticity, Fundamentals and Applications, COMPLAS VIII*, Barcelona, Spain.
- Simo, J. C., J. Oliver, and F. Armero (1993). An analysis of strong discontinuities induced by strain-softening in rate-independent inelastic solids. *Computational Mechanics* 12, 277–296.
- Simo, J. C. and M. S. Rifai (1990). A class of mixed assumed strain methods and the method of incompatible modes. *International Journal for Numerical Methods in Engineering* 29(8), 1595–1638.
- Simone, A. (2003). *Continuous-discontinuous modelling of failure*. Ph. D. thesis, Delft University of Technology.
- Simone, A. (2004). Partition of unity-based discontinuous elements for interface phenomena: computational issues. *Communications in Numerical Methods in Engineering*. 20, 465–468.
- Simone, A., G. N. Wells, and L. J. Sluys (2003). From continuous to discontinuous failure in a gradient-enhanced continuum damage model. *Computer Methods in Applied Mechanics and Engineering* 192(41–42), 4581–4607.
- Wells, G. (2001). *Discontinuous modelling of strain localisation and failure*. Ph. D. thesis, Delft University of Technology.
- Wells, G. N. and L. J. Sluys (2001). A new method for modelling cohesive cracks using finite elements. *International Journal for Numerical Methods in Engineering* 50(2), 2667–2682.